NASA/TM–2016–218975

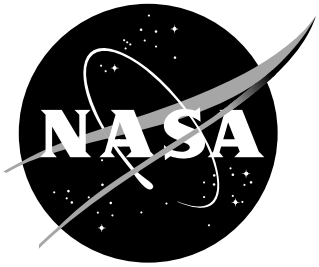

Pultruded Rod/Overwrap Testing for Various Stitched Stringer Configurations

Frank A. Leone, Jr.
NASA Langley Research Center, Hampton, VA

April 2016

NASA STI Program ... in Profile

Since its founding, NASA has been dedicated to the advancement of aeronautics and space science. The NASA scientific and technical information (STI) program plays a key part in helping NASA maintain this important role.

The NASA STI Program operates under the auspices of the Agency Chief Information Officer. It collects, organizes, provides for archiving, and disseminates NASA's STI. The NASA STI Program provides access to the NTRS Registered and its public interface, the NASA Technical Reports Server, thus providing one of the largest collections of aeronautical and space science STI in the world. Results are published in both non-NASA channels and by NASA in the NASA STI Report Series, which includes the following report types:

- TECHNICAL PUBLICATION. Reports of completed research or a major significant phase of research that present the results of NASA programs and include extensive data or theoretical analysis. Includes compilations of significant scientific and technical data and information deemed to be of continuing reference value. NASA counterpart of peer-reviewed formal professional papers, but having less stringent limitations on manuscript length and extent of graphic presentations.
- TECHNICAL MEMORANDUM. Scientific and technical findings that are preliminary or of specialized interest, e.g., quick release reports, working papers, and bibliographies that contain minimal annotation. Does not contain extensive analysis.
- CONTRACTOR REPORT. Scientific and technical findings by NASA-sponsored contractors and grantees.
- CONFERENCE PUBLICATION. Collected papers from scientific and technical conferences, symposia, seminars, or other meetings sponsored or co-sponsored by NASA.
- SPECIAL PUBLICATION. Scientific, technical, or historical information from NASA programs, projects, and missions, often concerned with subjects having substantial public interest.
- TECHNICAL TRANSLATION. English-language translations of foreign scientific and technical material pertinent to NASA's mission.

Specialized services also include organizing and publishing research results, distributing specialized research announcements and feeds, providing information desk and personal search support, and enabling data exchange services.

For more information about the NASA STI Program, see the following:

- Access the NASA STI program home page at ***http://www.sti.nasa.gov***
- E-mail your question to help@sti.nasa.gov
- Phone the NASA STI Help Desk at 757-864-9658
- Write to:
  NASA STI Information Desk
  Mail Stop 148
  NASA Langley Research Center
  Hampton, VA 23681–2199

NASA/TM–2016–218975

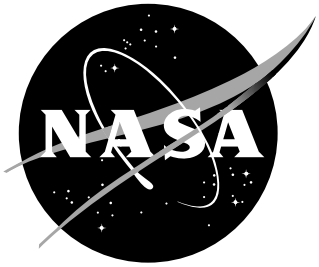

Pultruded Rod/Overwrap Testing for Various Stitched Stringer Configurations

Frank A. Leone, Jr.
NASA Langley Research Center, Hampton, VA

National Aeronautics and
Space Administration

Langley Research Center
Hampton, Virginia 23681-2199

April 2016

Acknowledgments

The author would like to acknowledge the contributions of Jonny Callahan for preparing the rod push-out specimens, Wade Jackson for performing the rod push-out specimen impacts, Gregory Shanks for setting-up and performing the rod push-out tests, and Peter Juarez and Patrick Johnston for performing the nondestructive evaluation of the stringer segments.

Abstract

The unidirectional carbon pultruded rod running through the tops of the stringers is a key design feature of the Pultruded Rod Efficient Unitized Structure (PRSEUS) concept as applied to aircraft fuselage structure. Reported herein are the test methods and results from a test campaign in which the strength of the rod/overwrap interface of various PRSEUS stringer configurations were characterized. The different stringer configurations included different materials and stacking sequences for the stringer overwrap and whether or not an additional layer of adhesive was included between the rod and the overwrap.

Contents

List of Figures

1 Introduction

As part of the NASA Environmentally Responsible Aviation (ERA) Project, researchers at NASA Langley Research Center (LaRC) and The Boeing Company (Boeing) worked together to develop technology to support lighter, more fuel-efficient commercial transport aircraft. A major milestone for the ERA Project was to design, build and test a 30-foot-long Multi-Bay Box (MBB) test article that was representative of an 80%-scale center section of a Hybrid Wing Body (HWB) vehicle. A sketch of the MBB with the forward upper and lower bulkhead panels removed is shown in figure 1. A detailed description of the steps in the multi-year process to develop this new lightweight composites concept is presented in reference 1.

The MBB test article contained 11 large, out-of-autoclave cured, carbon/epoxy panels built using the Pultruded Rod Stitched Efficient Unitized Structure (PRSEUS) concept [2]. PRSEUS is an enabling technology for the HWB architectures, due to the ability of the concept to support a pressurized, non-circular fuselage efficiently for both cost and weight. The primary motivation for the MBB development and testing was to demonstrate both the manufacturability for large-scale components and the performance and strength of the structure [3]. This new approach exploits the advantages of stitched composites by integrating the skin, frames, stringers, tear straps, and T-caps together into a single dry, self-supporting preform assembly. The integrated preform is then infused and co-cured in a single oven cure step using a vacuum-assisted resin transfer molding process with high-precision Invar outer mold line (OML) tooling. An exploded view of the intersection of a PRSEUS frame and stringer is shown in figure 2. Further details of the fabrication methodology for stitched composites are presented in reference 4.

The 11 stitched panels of the MBB test article were fabricated by Boeing at their facility in Huntington Beach, Calif., and subsequently assembled into the MBB at the Boeing C-17 final assembly facility in Long Beach, Calif. The MBB was tested in the Combined Loads Test System (COLTS) at LaRC in April through June 2015. The MBB was subjected to combinations of internal pressure loading and mechanical loading that were representative of the design limit loads and design ultimate loads of an HWB aircraft for various critical flight conditions. Testing of the MBB is documented in reference 5.

During fabrication of the panels for the MBB, ideas were developed about how to improve the design and further develop stitched structure for future applications. Therefore, an additional panel was fabricated to test some of these ideas. The primary motivation for fabricating this additional panel was to evaluate the structural performance of different configurations of the frames, stringers, and T-caps, as well as to develop the necessary fabrication processes and procedures for these new configurations.

This report focuses on a set of stringer rod push-out specimens that were harvested from an alternate center keel panel. This report presents details regarding the test specimens, the experimental procedure that was used to evaluate the specimens, and a discussion of the experimental results. These push-out specimens and tests are similar to those reported in reference 6. Separate reports are available which focus on the testing and evaluations of the different T-cap configurations [7] and a series of single-frame and single-stringer compression tests [8] which were harvested from the additional PRSEUS panel.

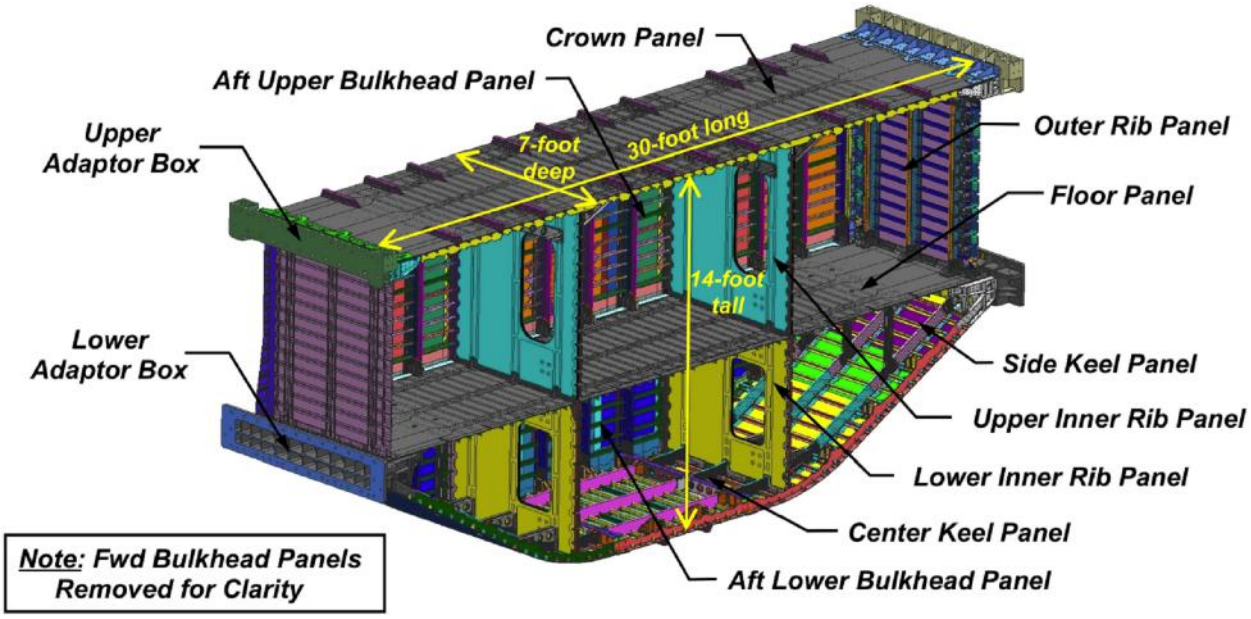

Figure 1: MBB test article components.

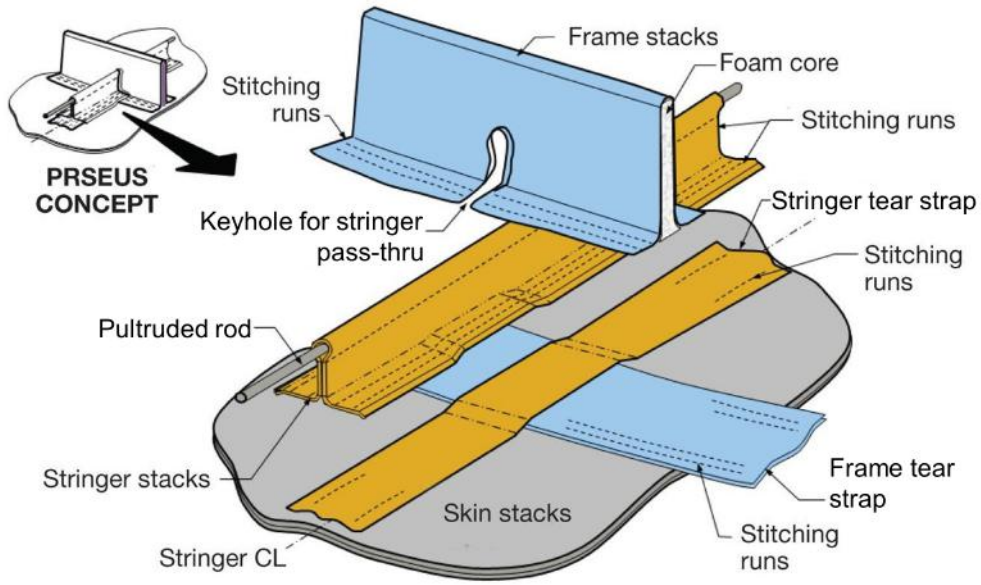

Figure 2: PRSEUS concept components.

2 Alternate Center Keel

A second center keel panel, based on the MBB center keel panel, was fabricated by Boeing and delivered to LaRC in February 2015. The inner mold line (IML) surface of this alternate MBB center keel panel is shown in figure 3. The panel measured 71.9 inches long and 75.4 inches wide. The panel was made from a combination of dry carbon warp-knit fabric, pultruded rods, foam core, and stitching threads.

The skin and most parts of the stiffeners were made from carbon fiber layers with a stacking sequence of $[+45/-45/0/90/0/-45/+45]$. This material grouping, known as Class 72, Type 1 pre-kitted stacks, was the same material used in the MBB [2]. Each of these stacks has a nominal cured thickness of 0.052 inches. Standard modulus Toho HTA40E13 carbon fibers were used in the Class 72 stacks. A second material grouping, known as Class 101, Type 3, was included in the alternate center keel panel. The Class 101 pre-kitted stacks have a stacking sequence of $[+30/0/-30/0]$ and nominal cured thickness of 0.021 inch. IMS65 E23, Toho Tenax-E 24K intermediate modulus fibers were used in the Class 101 stacks. Multiple stacks of the warp-knit materials were used to build up the desired part stiffness, strength, and configuration.

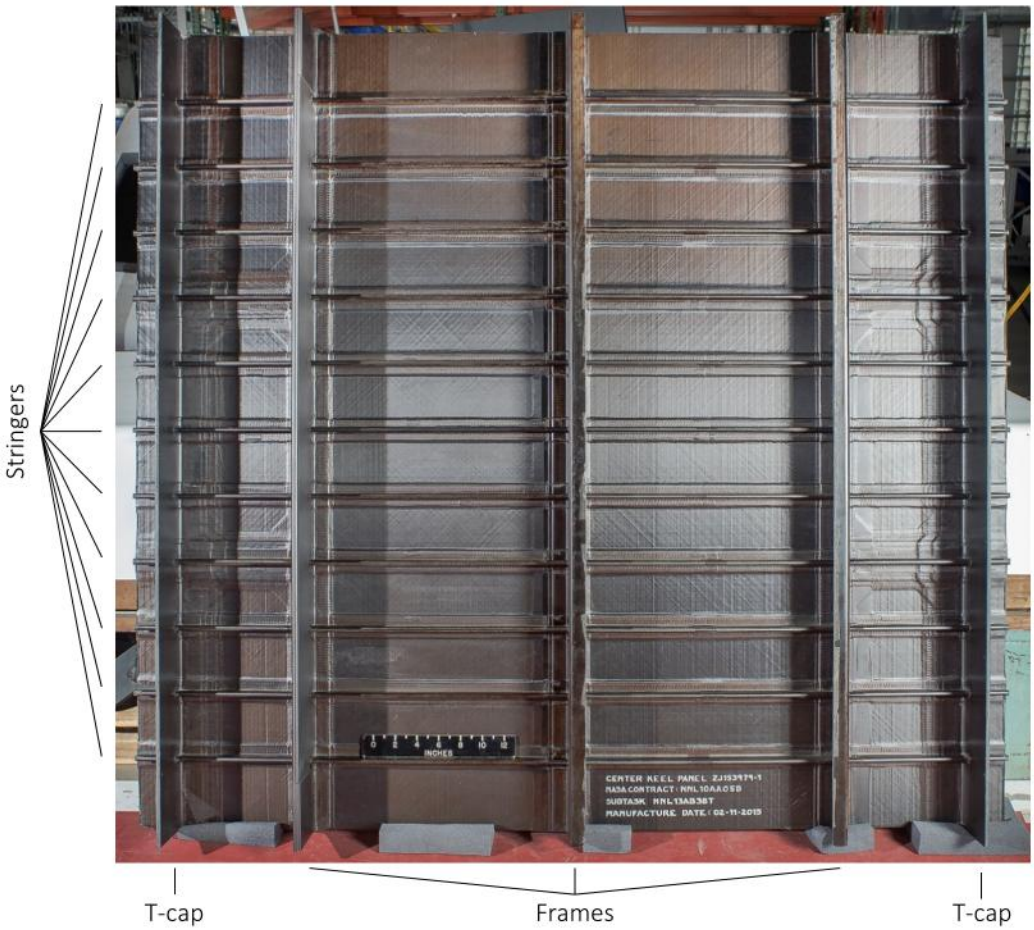

Figure 3: Photograph of the IML surface of the MBB alternate center keel panel, showing the stringers, frames, and T-caps.

Through-the-thickness stitching was used to attach the stiffeners to the skin and, in selected locations, in the stiffener webs to form a dry, self-supporting preform. The preform was then infused with VRM-34 epoxy resin and cured in an oven. The completed stiffened panel contained three frames, 11 stringers, and two T-caps. Additional details regarding the design and fabrication of the alternate MBB center keel panel can be found in reference 9.

2.1 Stringer Configurations

A PRSEUS stringer consists of a tear-shaped, unidirectional, carbon rod contained within a carbon/epoxy overwrapping laminate. The overwrapping laminate also forms the web and bottom flange of the stringer. A schematic representation of a typical PRSEUS stringer cross-section which highlights each of these features is shown in figure 4. Five different stringer configurations were included in the alternate center keel panel, as shown in figure 5. The five stringer configurations varied in terms of stack material, stack orientation, and whether or not an adhesive layer was included between the rod and the overwrap:

- Class 72 overwrap (labeled S07, S10, S11);
- Class 72 overwrap with adhesive between the rod and overwrap (labeled S08, S09);
- Class 101 overwrap (labeled S01, S02, S05);
- Class 101 overwrap with adhesive between the rod and overwrap (labeled S03, S04); and
- Class 101 overwrap with a reversed stacking sequence (labeled S06).

The adhesive used between the rod and the overwrap in stringers S03, S04, S08, and S09 was Cytec FM300 adhesive. The layer of adhesive was 0.015 inch thick.

The default configuration of the Class 101 stacks (i.e., S02 through S05) had the outer 0° fibers placed against the rod. The reversed stacking sequence (i.e., S06) had the +30° fibers placed against the rod. Stringer S06 was not used in this study due to being fully harvested for the single-stringer compression specimens [8].

The Class 72 stringers had two stacks (0.104 in.) in the web and one stack (0.052 in.) in the overwrap. The Class 101 stringers had four stacks (0.084 in.) in the web and two stacks (0.042 in.) in the overwrap. All of the stringer stacks were aligned in the 0° direction, with the 0° direction being aligned with the length of the stringers. The pultruded rods in the stringers were 0.375 inch

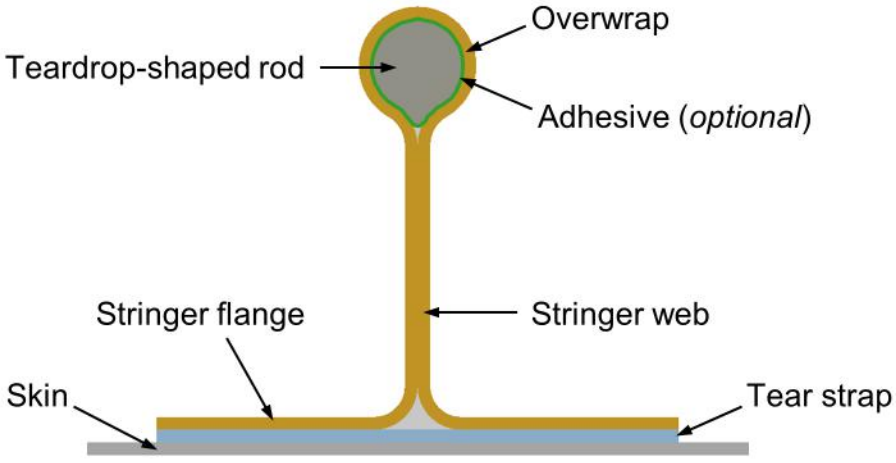

Figure 4: PRSEUS stringer cross-section.

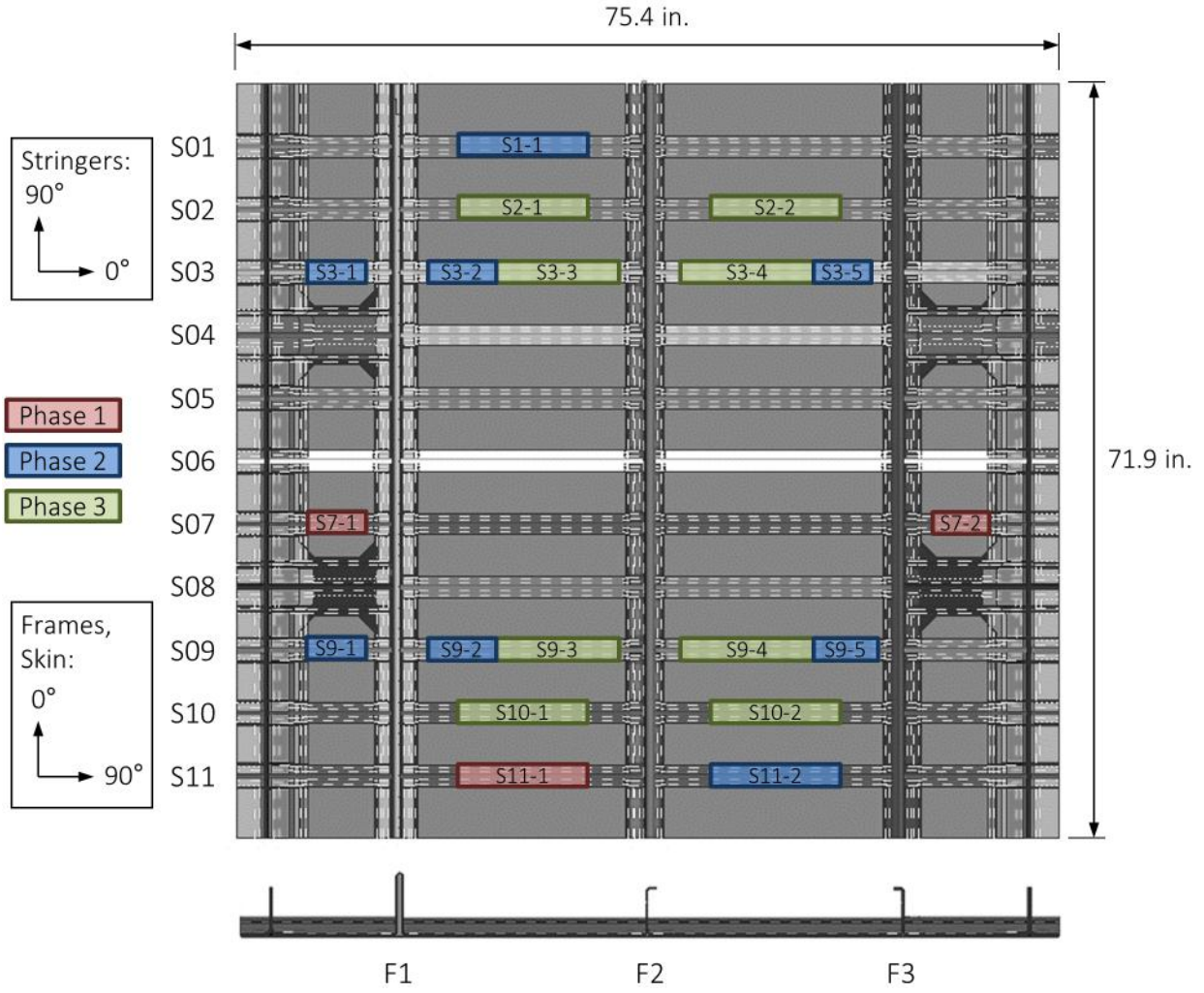

Figure 5: Alternate MBB center keel panel stringers which were harvested for stringer rod push-out test specimens.

in diameter, and composed of Grafil 34-700WD standard modulus carbon fibers and PUL6 epoxy resin, with a teardrop shape. Each stringer measured approximately 1.875 inches in height from the OML surface to the top of the stringer overwrap.

3 Experiment

The stringer rod push-out testing was divided into three phases. The first phase was used to size the specimens for the following two phases. In the second phase of testing, the strength of the interface between the pultruded rod and the overwrap was characterized for the four stringer configurations (i.e., Class 72 and Class 101, with and without adhesive). In the third phase of testing, the rod push-out specimens were impacted prior to testing, and the interface strength as a function of the distance from the impact site was characterized.

3.1 Specimen Preparation

Stringer rod push-out specimens were harvested from the alternate center keel panel from stringers S01, S02, S03, S07, S09, S10, and S11. Segments of stringers were cut from the panel, which varied in length from approximately 4 to 12 inches. The locations from which the stringer segments were taken in the alternate center keel panel are shown in figure 5. Each stringer segment was cut through the stringer web 1-7/16 inches from the top of the stringer overwrap. In this configuration, all of the stringer segments were immersed and scanned in an ultrasonic tank to assess the initial quality of the specimens—no major defects were found. The full length and the top 120 degrees of each segment were scanned. The stringer segments were then cut down into shorter stringer rod push-out specimens. In phase one, specimen lengths of 0.5 inch, 1.0 inch, and 2.0 inches were evaluated. The specimens in phases two and three were all 1.0 inch in length.

After being cut to length, the stringer rod push-out specimens were potted in an aluminum tool using Hysol EA 9394 paste adhesive. The aluminum tools each held five stringer rod push-out specimens. The tools were 0.5 inch deeper than the specimen length (i.e., 1.5 inches deep during phases two and three). The specimens were set and potted in the top of the aluminum tools. A 0.60-inch-diameter hole was drilled through the tool to be concentric with the specimen rods to allow the rod to push through. An example of a prepared set of stringer rod push-out specimens is shown in figure 6. A steel teardrop-shaped button was glued to the top of each specimen rod to allow for more uniform load introduction to the rod/overwrap interface. The steel button had the same shape as the rods, but was slightly undersized so as to only be in contact with the rod.

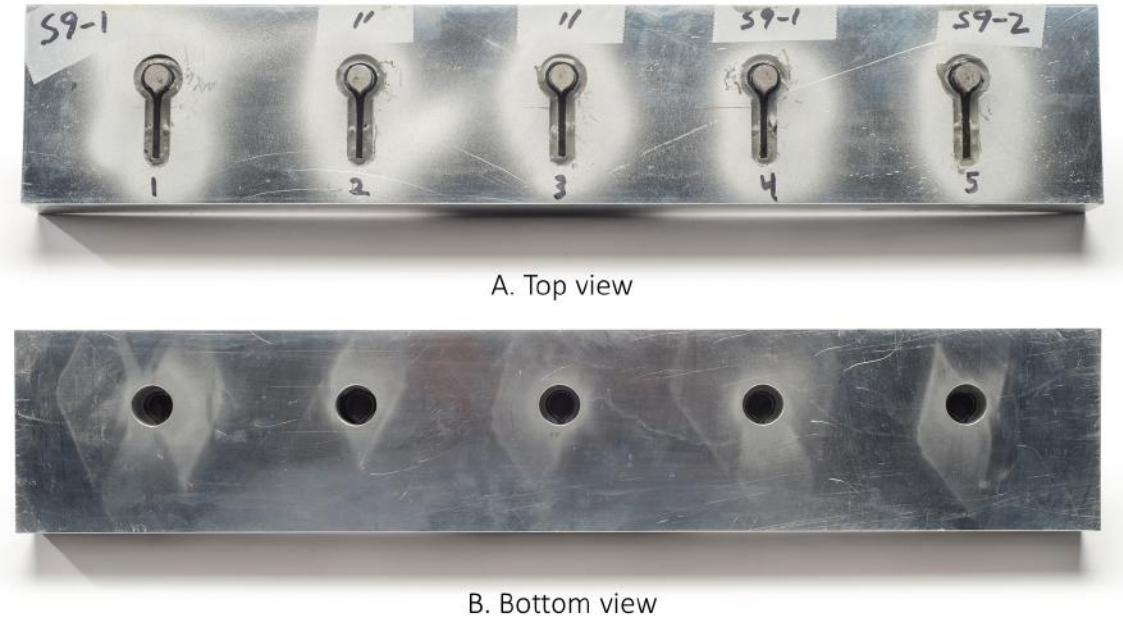

Figure 6: Stringer rod push-out specimens potted in the aluminum tool.

3.2 Impacts

After their initial ultrasound scan, eight stringer segments from which the phase three specimens would be cut were impacted. The stringer segments were impacted on the top of the stringer

rod overwrap using drop-weight impactor with a 1-inch-diameter spherical indenter. The indenter assembly weighed 3.7 lb. Each of the specimens was impacted with a nominal 21.2 ft-lb impact energy. The energy of the actual impacts was measured to be approximately 19 ft-lb.

During the impacts, the stringer segments were supported in a pinned-pinned configuration. To have the stringer segments oriented vertically during the impacts, two 0.375-inch-diameter holes were drilled 11.5 inches apart center-to-center in the stringer web. Two 0.375-inch bolts were installed through the holes to allow the specimen to ride along two rails, which were formed by two adjacent I-beams on their sides, as shown in figure 7.

No visible damage was observed after the impacts. However, an additional round of nondestructive evaluations via ultrasound inspection revealed substantial subsurface damage.

After being scanned a second time, the eight impacted stringer segments were each sectioned into nine 1.0-inch-long specimens, with the fifth specimen from each segment being centered on the impact site.

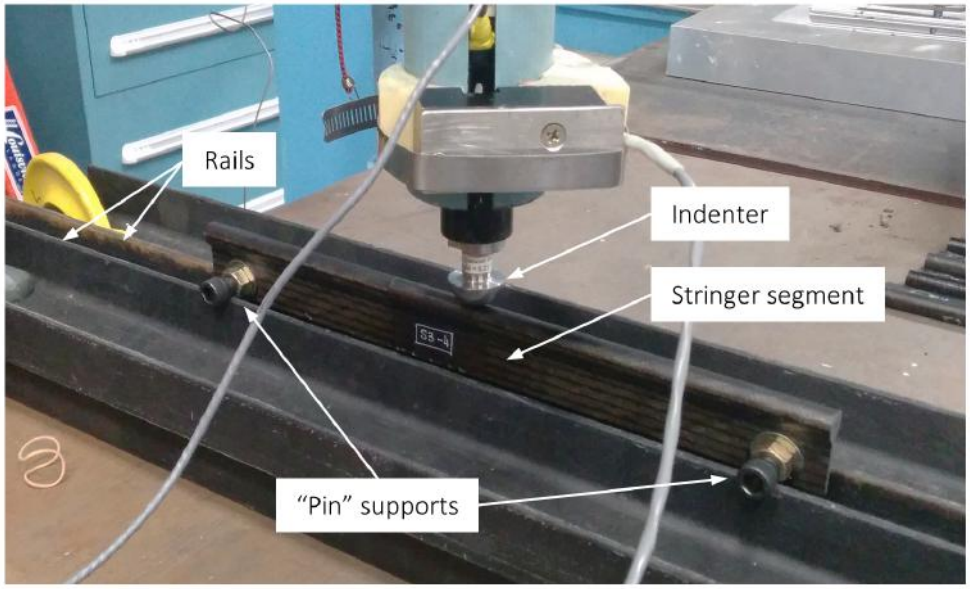

Figure 7: Phase three stringer segment impact setup.

3.3 Testing

The stringer rod push-out specimens were tested on a 20 kip load frame at NASA LaRC. All tests were conducted at room temperature. The specimens were quasi-statically, monotonically loaded to failure under displacement control. A stroke rate of 0.01 inch/minute was used.

A modified 5/8-inch bolt was used as the indenter for the tests, as shown in figure 8a. The diameter was reduced to 0.480 inch at the bottom of the bolt, and the bottom was cut flat so as to uniformly compress the steel buttons attached to the rods in the specimens. The displacement of the rod was measured with a linear variable displacement transducer (LVDT) placed underneath the specimen tray. The LVDT measured the displacement of the rod through the 0.60-inch-diameter hole in the aluminum tool through which the rods were pushed. The displacement of the overwrap was measured from the top of the specimen using an MTS 632.06H-31 displacement gauge. The

overwrap displacement gauge had a custom adapter which contacted the overwrap at two points on either side of the steel button, as shown in figure 8b.

Load, displacement, and stroke data were recorded at a rate of 10 Hz during the tests. The rod and overwrap displacement readings were zeroed before each test.

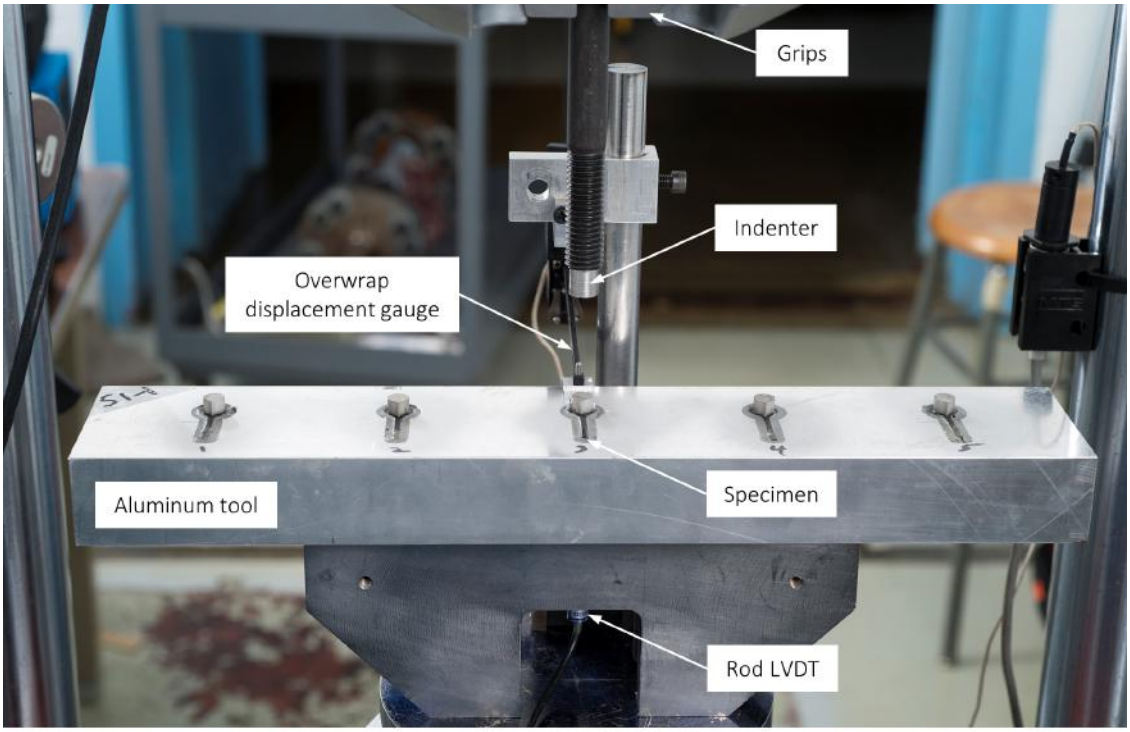

A. Load frame view

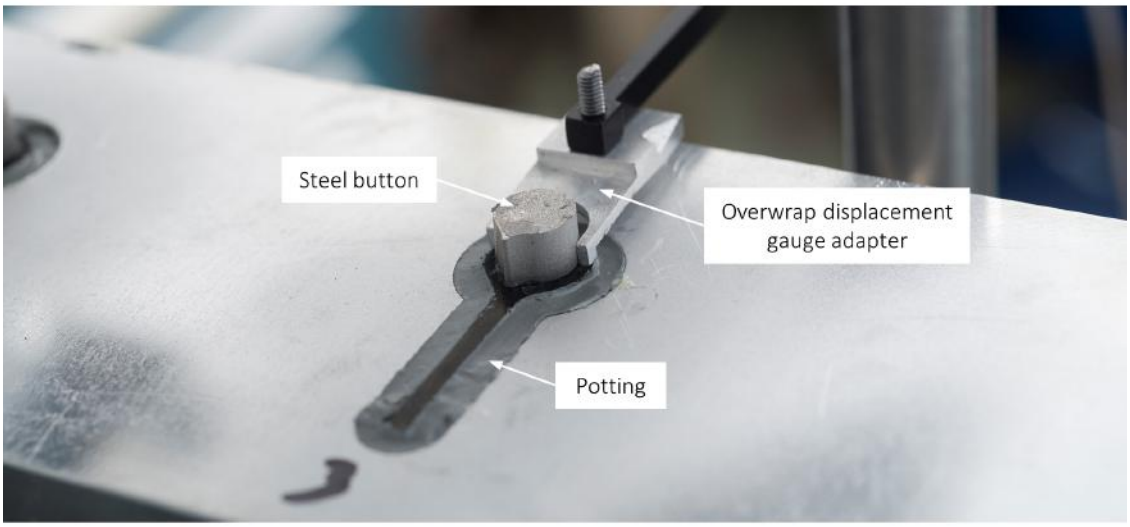

B. Specimen view

Figure 8: Experimental setup for stringer rod push-out tests.

4 Results and Discussion

Among the rod push-out specimens tested throughout this program, differences in peak load, failure location, and load-displacement response between and within specimen configurations were recorded. In addition, a significant amount of friction between the overwrap and the rod occurred during and after specimen failure. As a result, the definition of specimen's ultimate failure load was not as straightforward as noting the peak load before a significant load drop. As a result, the overwrap and rod displacement results were used to define a failure condition. A specimen was considered to have failed after the time rate of change of the rod displacement approached the stroke rate and the time rate of change of the overwrap displacement approached zero. A schematic showing the stroke, rod displacement, and overwrap displacement behavior during the failure process is shown in figure 9. The specimen shear strength is herein defined as the load divided over the rod/overwrap interface at the time of failure, as defined above.

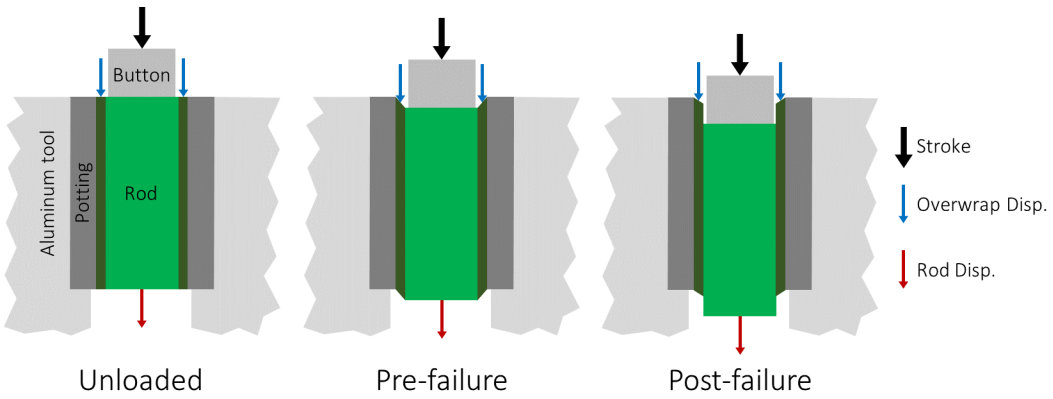

Figure 9: Schematic of cross-sectional view of the rod and overwrap displacements during failure process.

4.1 Phase One

Five replicates of 0.5-, 1.0-, and 2.0-inch-long specimens were tested during phase one. All of the tested specimens were composed of Class 72 material and contained no adhesive at the rod/overwrap interface.

The shear strength results obtained during phase one are reported in table 1. The mean strength results for the three specimen lengths tested were similar, with significant overlap between the ranges of strengths recorded for each specimen length. All specimens failed at the rod/overwrap interface. There was no additional visible damage to either the rod or the overwrap in any of the specimens.

Of the three tested lengths, the 1.0-inch-long specimen configuration was selected for the phase two and phase three specimens since they had the lowest standard deviation. In addition, the process of uniformly potting the 2.0-inch-long specimens was much more difficult than for the shorter specimens, which eliminated the 2.0-inch-long specimen configuration from consideration.

Table 1: Phase one results: shear strength versus specimen length.

Replicate	0.5 inch [psi]	1.0 inch [psi]	2.0 inch [psi]
1	1965	2444	2854
2	2768	2536	2416
3	1839	2648	2396
4	2841	2562	2274
5	2573	2476	1729
Mean	2397	2533	2334
Std. Dev.	19.4%	3.6%	17.3%

4.2 Phase Two

In the second phase of testing, four stringer configurations were evaluated, with ten 1.0-inch-long replicates of each stringer configuration. The four evaluated stringer configurations were Class 72, Class 72 with adhesive, Class 101, and Class 101 with adhesive. The shear strengths for all phase two specimens are listed in table 2 and plotted in figure 10.

After each test, the top and bottom surfaces of the specimen were visually inspected. Three different failure modes were observed amongst the phase two specimens. Photographs of the different failures modes are shown in figure 11, and the strength results in figure 10 are color-coded to indicate which failure mode was observed for each test. The three observed failure modes were:

1. rod/overwrap debonding,
2. failure along the adhesive bond, and
3. interlaminar delamination.

The rod/overwrap debonding failure mode was characterized by a clean break between the overwrap and the pultruded rod in specimens without adhesive, as shown in figure 11a. The second failure mode, failure along the adhesive bond, was observed for both the Class 72 and Class 101 configurations with adhesive. An example of a failure along the adhesive bond is shown in figure 11b. The third failure mode, interlaminar delamination, was observed for both the Class 72 and Class 101 specimens. In the Class 72 specimens, interlaminar delamination, when observed, occurred between the 90° and inner 0° plies of the overwrap. The Class 101 specimens which exhibited interlaminar delamination did not have a preferred interface in which to delaminate. An example of an interlaminar delamination failure for a Class 72 specimen is shown in figure 11c.

Because the visual inspections of the specimens were limited to the top and bottom surfaces, it was difficult to distinguish between adhesive failure between the adhesive and the overwrap, adhesive failure between the adhesive and the rod, and cohesive failure. However, the majority of specimens with this failure mode had adhesive visible along the interior of the overwrap on the top of the specimen and along the exterior of the rod on the bottom of the specimen, suggesting cohesive failure.

The Class 101 specimens without adhesive had an average shear strength 119% higher than the Class 72 specimens without adhesive, with strengths of 5.7 ksi and 2.6 ksi, respectively. Both the Class 72 and Class 101 specimens without adhesive exhibited primarily rod/overwrap debonding failure modes, with three of the ten Class 101 specimens exhibiting some interlaminar cracking as well, as is indicated in figure 10.

Table 2: Phase two results: shear strength versus configuration.

Replicate	C72 [psi]	C101 [psi]	C72+Adh [psi]	C101+Adh [psi]
1	2316	5564	2813	5533
2	2117	5062	3071	4922
3	2433	5796	2935	5399
4	2435	5724	2968	5524
5	2191	6026	3442	N/A
6	3225	6024	4114	4861
7	2761	6367	4122	5254
8	2553	5441	4167	5814
9	2689	6147	3273	5462
10	3358	5293	2822	5870
Mean	2608	5744	3373	5404
Std. Dev.	15.8%	7.1%	16.6%	6.4%

Including the adhesive layer in the Class 72 specimens resulted in a 31% increase in the average measured shear strength. In addition, two clearly different failure modes were observed, interlaminar delamination and failure along the adhesive bond, which corresponded to different average shear strengths. The seven specimens which failed via interlaminar delamination had an average shear strength of 3.0 ksi and a standard deviation of 7.7%, 15% higher than the Class 72 specimens without adhesive. The three specimens which failed along the adhesive bond, however, had an average shear strength of 4.1 ksi and a standard deviation of 0.7%, 58% higher than the Class 72 specimens without adhesive. The inclusion of the adhesive layer in the Class 101 specimens caused a 5% decrease in the average measured shear strength, but this difference is less than the standard deviation of the two data sets.

The load-displacement histories of the phase two specimens are plotted in figure 12. The Class 72 specimens without adhesive, shown in figure 12a, all exhibited the same rod/overwrap debonding failure mode, and had similar load-displacement responses. The specimen load-displacement histories were linear up to -3 kips applied load, after which either failure or a gradual decrease in the slope of the response occurred. Failure for all Class 72 specimens without adhesive was brittle, with a large, sudden load drop.

The Class 72 specimens with adhesive, shown in figure 12b, had different load-displacement history types for the two failure modes that were exhibited during the tests. The specimens which failed via interlaminar delamination had a stick/slip type of behavior, characterized by several small load drops and decreasing load-displacement slope. The specimens which failed along the adhesive bond failed in a ductile style, with stable decrease in load from the peak load, followed by reaching a constant-load plateau. This load plateau is caused by friction resisting the push-out of the rod through the overwrap.

The Class 101 specimens without adhesive, shown in figure 12c, exhibited the same brittle failure behavior as the Class 72 specimens. Nonlinearity in the load-displacement responses began at a much lower percent of the average failure load than for the Class 72 specimens.

The Class 101 specimens with adhesive, shown in figure 12d, exhibited two different load-

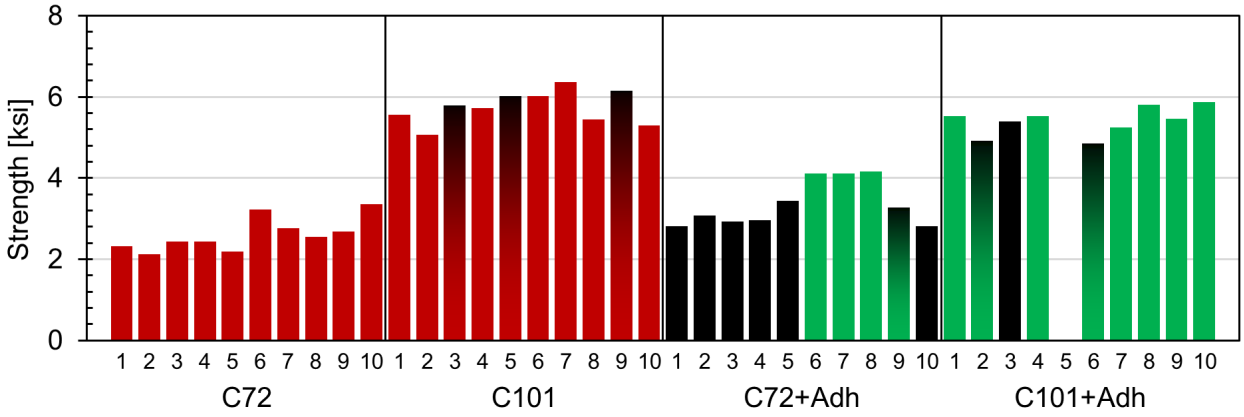

Figure 10: Phase two stringer rod push-out shear strengths and failure modes. Red indicates rod/overwrap debonding, green indicates failure along the adhesive bond, and black indicates interlaminar delamination. Gradients indicate mixed-mode failure.

Figure 11: Types of failure observed in the stringer rod push-out specimens.

displacement behaviors, corresponding to the two different observed failure modes. The specimens which failed via interlaminar delamination underwent brittle failure. The specimens which failed along the adhesive bond had stable reductions in load after the peak load, unloading to a consistent load plateau which corresponds to the friction force required to push out the rod.

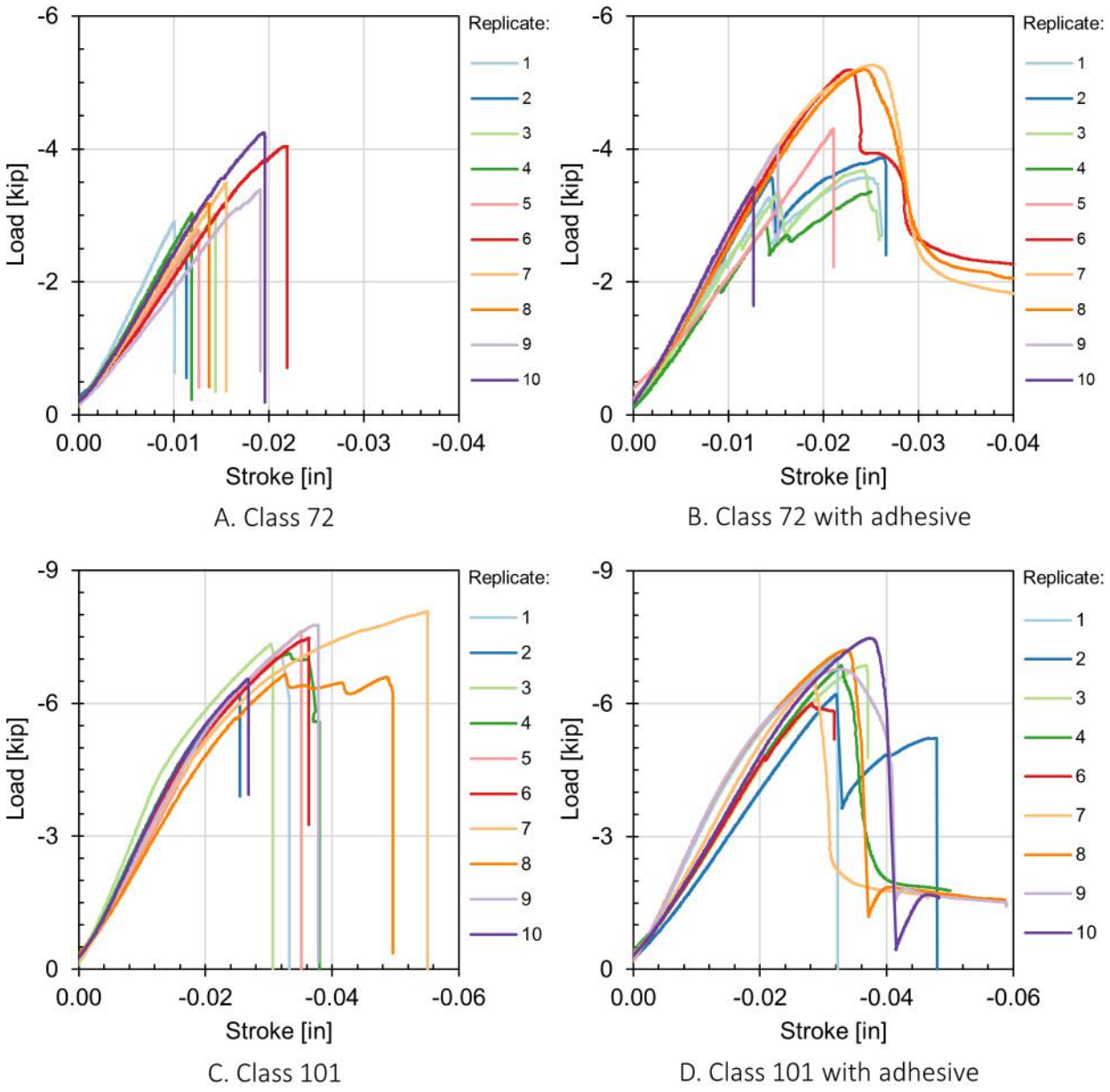

Figure 12: Phase two stringer rod push-out specimen load-displacement responses.

4.3 Phase Three

The phase three tests provided strength data versus distance from the impact location of the stringer segments. In addition, ultrasonic scans of the stringer segments after being impacted provided a map of the subsurface damage prior to testing. The ultrasonic inspection and shear strength data as a function of push-out specimen position along the stringer segment length are provided in figures 13 through 16. The dimensions of the scanned areas in the ultrasonic scan images in these figures is 9.5 inches by 0.50 inch for the Class 72 specimens and 9.5 inches by 0.48 inch for the Class 101 specimens.

Damage extended one to two inches in each direction from the impact location in the two impacted Class 72 specimens without adhesive, shown in figure 13. The specimens cut from the regions where damage was detected had strengths below the range of the phase two results, with the lowest strengths being recorded for the specimens which contained the impact location. Visual inspection of the top and bottom of the tested specimens revealed that the dominant failure mode was rod/overwrap debonding, consistent in mode with the phase two results.

The two impacted Class 72 specimens with adhesive, shown in figure 14, did not have similar damaged areas. The delaminated area in the first impacted stringer segment extended from the impact location to one side of the stringer segment. The second stringer segment, instead, had its damage highly localized at the impact site. The strength results for the first stringer segment were all comparable to the phase two results. The measured strengths for the second stringer segment was less than the phase two average for the specimen that included the impact site and one adjacent specimen. All but one of the impacted Class 72 specimens with adhesive exhibited interlaminar delamination.

The two impacted Class 101 specimens without adhesive had damage localized to the impact locations, as detected via ultrasonic inspection, shown in figure 15. In both impacted stringer segments, the damage extended only one inch along the stringer length. However, along the circumference of the overwrap, the damage extended beyond the 120° arc which was inspected. The measured strengths for the first stringer segment specimens were constant along the stringer segment length, with no significant drop at the impact site, though the strengths were consistently below the phase two average. The measured strengths for the second stringer segment specimens were all well below the phase 2 average results, with the lowest measured strengths being measured closest to the center of the stringer segment. For both the first and second stringer segment specimens, the observed failure mode was rod/overwrap debonding.

The two impacted Class 101 specimens with adhesive had similar damage states, extending one to three inches along the top of the stringer rod overwrap, and propagating further along the circumference of the rod overwrap along the ±30° fiber directions, as shown in figure 16. The measured strengths did trend with the severity of the measured damage, though only slightly. The strength results were generally consistent along the stringer segment lengths, on average 63% of the phase 2 average strength. Interlaminar delamination was the dominant observed failure mode.

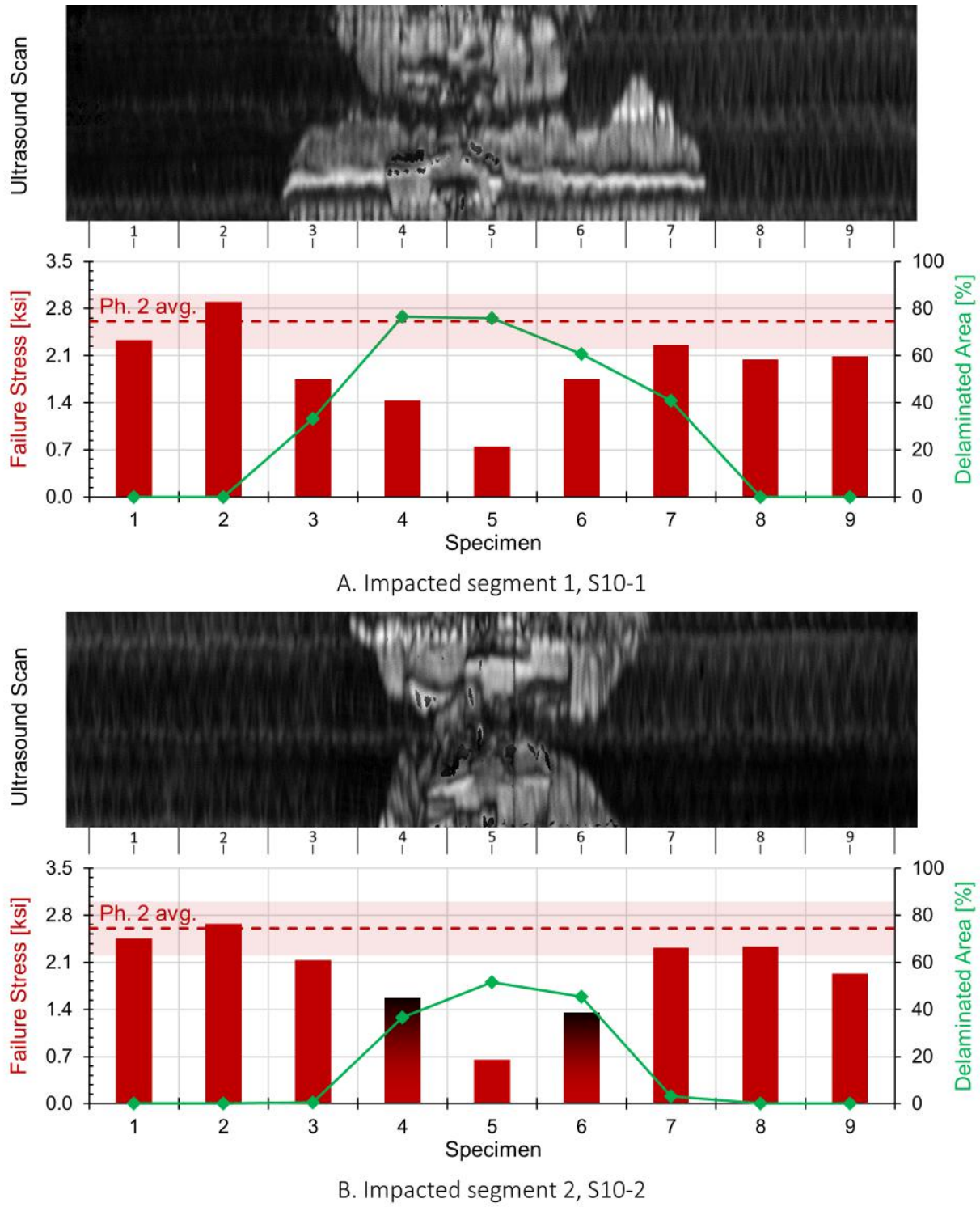

Figure 13: Ultrasound scan and distribution of strengths for impacted Class 72 specimens without adhesive. Red indicates rod/overwrap debonding and black indicates interlaminar delamination.

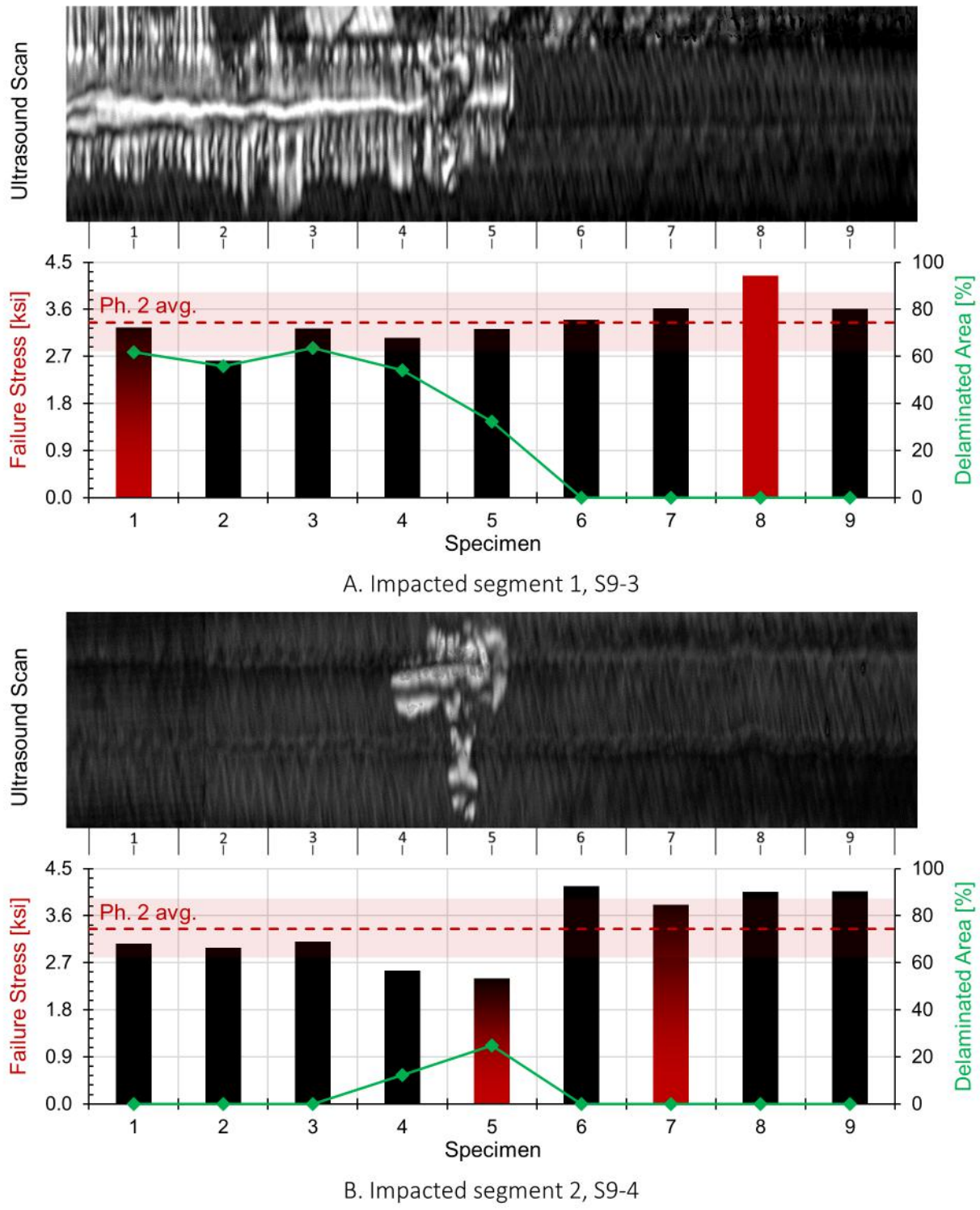

Figure 14: Ultrasound scan and distribution of strengths for impacted Class 72 specimens with adhesive. Red indicates failure along the adhesive bond and black indicates interlaminar delamination.

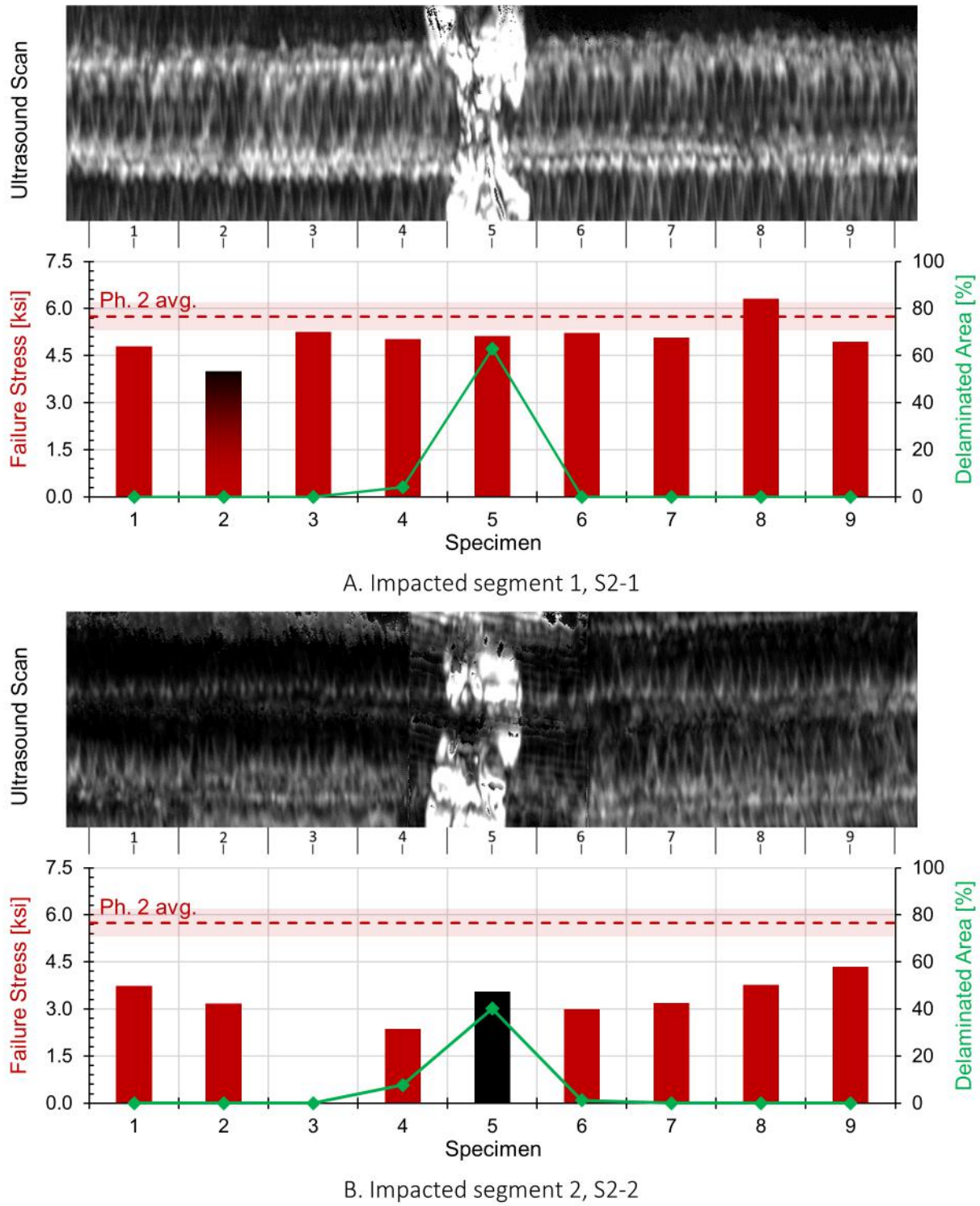

Figure 15: Ultrasound scan and distribution of strengths for impacted Class 101 specimens without adhesive. Red indicates rod/overwrap debonding and black indicates interlaminar delamination.

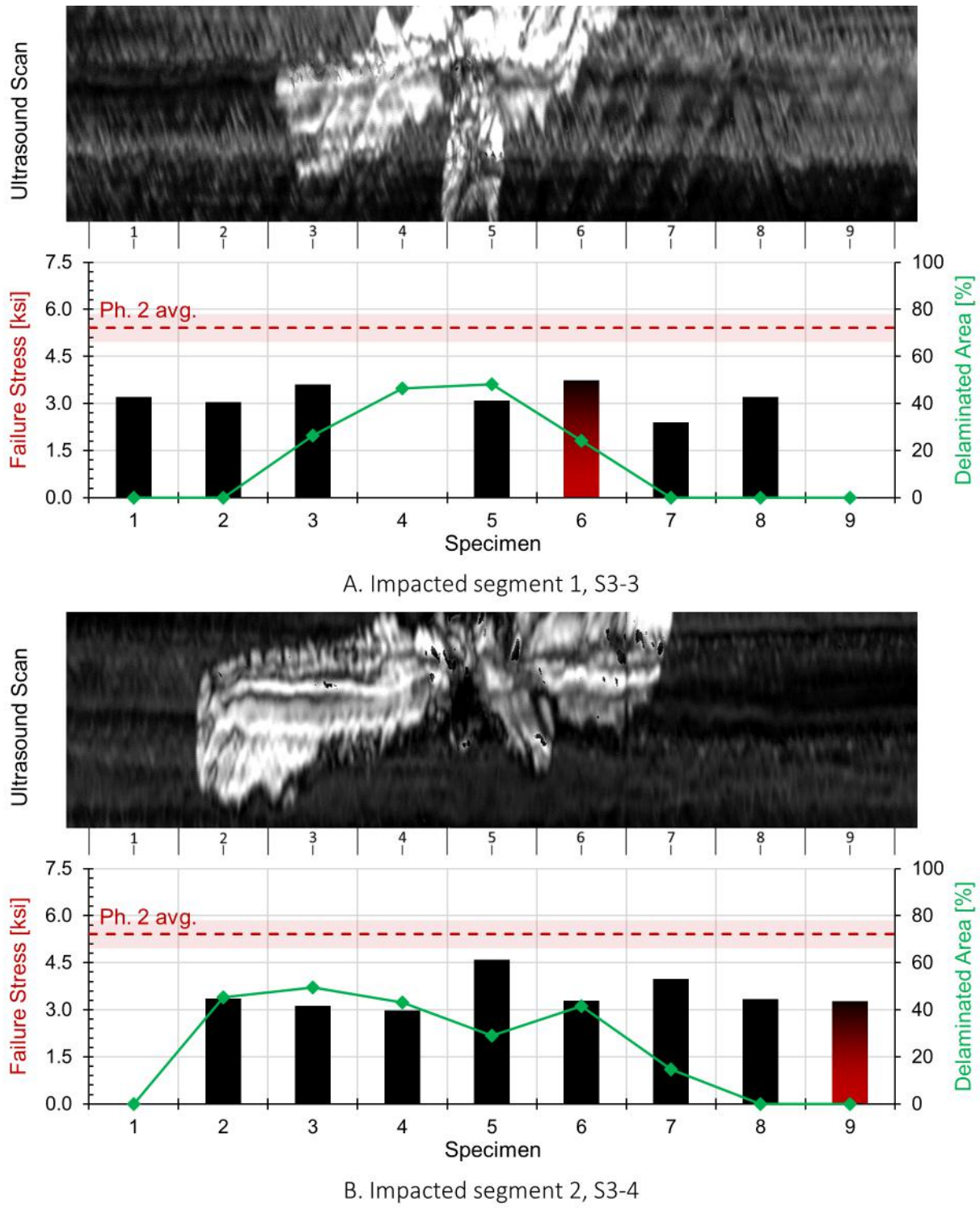

Figure 16: Ultrasound scan and distribution of strengths for impacted Class 101 specimens with adhesive. Red indicates failure along the adhesive bond and black indicates interlaminar delamination.

5 Concluding Remarks

A series of tests were conducted in which the unidirectional pultruded rod of a PRSEUS stringer was pushed-out through its overwrapping stacks of carbon/epoxy material. Four different specimen configurations were evaluated, including two different overwrap configurations and specimens with and without a layer of adhesive located between the overwrap and the rod. The specimens were tested in impacted and non-impacted states. These are non-standard tests, and a continuation of previous PRSEUS characterization studies.

In general, the stringers with the Class 101 overwrap had much higher interfacial strengths between the rod and the overwrap than the specimens with the Class 72 overwrap. The inclusion of adhesive between the rod and the overwrap increased the measured interfacial strength for the specimens with the Class 72 overwrap, but did not cause any improvement in the performance of the Class 101 specimens. The inclusion of the adhesive layer in the Class 72 specimens changed the failure mode of the specimens from debonding of the overwrap and the rod to either failure along the adhesive bond or interlaminar delamination in the overwrap material.

In response to impact, the Class 72 specimens had reduced strengths in the regions in which damage was detected by ultrasonic inspection, as expected. The measured strengths of the impacted Class 101 specimens did not clearly trend with the severity of the measured damage along the stringer length. Instead, the Class 101 specimens from a single impacted stringer segment had uniform, reduced strengths along its length, with the strength reduction with respect to the average non-impacted strength not trending clearly with the amount of damage measured via ultrasound.

References

1. Jegley, D.; and Velicki, A.: Status of Advanced Stitched Unitized Composite Aircraft Structure. *51st AIAA Aerospace Sciences Meeting including the New Horizons forum and Aerospace Exposition*, Grapevine, Tex., Jan. 2013.

2. Velicki, A.: Damage Arresting Composites for Shaped Vehicles, Phase I Final Report. NASA/CR-2009-215932, NASA Langley Research Center, Hampton, Va., Sept. 2009.

3. Velicki, A.; Yovanof, N.; Baraja, J.; Linton, K.; Li, V.; Hawley, A.; Thrash, P.; DeCoux, S.; and Pickell, R.: Damage Arresting Composites for Shaped Vehicles—Phase II Final Report. NASA/CR-2011-216880, NASA Langley Research Center, Hampton, Va., Jan. 2011.

4. Linton, K.; Velicki, A.; Hoffman, K.; Thrash, P.; Pickell, R.; and Turley, R.: PRSEUS Panel Fabrication Final Report. NASA/CR-2014-218149, NASA Langley Research Center, Hampton, Va., Jan. 2014.

5. Jegley, D.; Rouse, M.; Przekop, A.; and Lovejoy, A.: The Behavior of a Stitched Composite Large-Scale Multi-Bay Pressure Box. NASA/TM-2016-218972, NASA Langley Research Center, Hampton, Va., 2016.

6. Wang, J.; Grenoble, R.; and Pickell, R.: Structural Integrity Testing Method for PRSEUS Rod-Wrap Stringer Design. *53rd AIAA/ASME/ASCE/AHS/ASC Structures, Structural Dynamics and Materials Conference*, Honolulu, Hawaii, Apr. 2012.

7. Lovejoy, A.; and Leone, F.: T-cap Pull-off and Bending Behavior for Stitched Structure. NASA/TM-2016-218971, NASA Langley Research Center, Hampton, Va., 2016.

8. Leone, F.; and Jegley, D.: Compressive Testing of Stitched Frame and Stringer Alternate Configurations. NASA/TM-2016-218974, NASA Langley Research Center, Hampton, Va., 2016.

9. Velicki, A.; Hoffman, K.; Linton, K.; Thrash, P.; Pickell, R.; and Turley, R.: Fabrication of Lower Section and Upper Forward Bulkhead Panels of the Multi-Bay Box and Panel Preparation. NASA/CR-2015-218981, NASA Langley Research Center, Hampton, Va., Nov. 2015.

REPORT DOCUMENTATION PAGE

Form Approved
OMB No. 0704-0188

1. REPORT DATE *(DD-MM-YYYY)*	2. REPORT TYPE	3. DATES COVERED *(From - To)*
01-04-2016	Technical Memorandum	

4. TITLE AND SUBTITLE

Pultruded Rod/Overwrap Testing for Various Stitched Stringer Configurations

5a. CONTRACT NUMBER

5b. GRANT NUMBER

5c. PROGRAM ELEMENT NUMBER

6. AUTHOR(S)

Leone, Frank A.

5d. PROJECT NUMBER

5e. TASK NUMBER

5f. WORK UNIT NUMBER

338881.02.22.07.01.01

7. PERFORMING ORGANIZATION NAME(S) AND ADDRESS(ES)

NASA Langley Research Center
Hampton, VA 23681-2199

8. PERFORMING ORGANIZATION REPORT NUMBER

L-20632

9. SPONSORING/MONITORING AGENCY NAME(S) AND ADDRESS(ES)

National Aeronautics and Space Administration
Washington, DC 20546-0001

10. SPONSOR/MONITOR'S ACRONYM(S)

NASA

11. SPONSOR/MONITOR'S REPORT NUMBER(S)

NASA-TM-2016-218975

12. DISTRIBUTION/AVAILABILITY STATEMENT

Unclassified - Unlimited
Subject Category 24
Availability: NASA STI Program (757) 864-9658

13. SUPPLEMENTARY NOTES

14. ABSTRACT

The unidirectional carbon pultruded rod running through the tops of the stringers is a key design feature of the Pultruded Rod Efficient Unitized Structure (PRSEUS) concept as applied to aircraft fuselage structure. Reported herein are the test methods and results from a test campaign in which the strength of the rod/overwrap interface of various PRSEUS stringer configurations were characterized. The different stringer configurations included different materials and stacking sequences for the stringer overwrap and whether or not an additional layer of adhesive was included between the rod and the overwrap.

15. SUBJECT TERMS

PRSEUS; Pultruded rod; Stringers; adhesive

16. SECURITY CLASSIFICATION OF:			17. LIMITATION OF ABSTRACT	18. NUMBER OF PAGES	19a. NAME OF RESPONSIBLE PERSON
a. REPORT	b. ABSTRACT	c. THIS PAGE			STI Help Desk (email: help@sti.nasa.gov)
					19b. TELEPHONE NUMBER *(Include area code)*
U	U	U	UU	29	(757) 864-9658